2017 American Control Conference
Sheraton Seattle Hotel
May 24–26, 2017, Seattle, USA

The Elusive Consequences of Slow Engine Response on Drive Cycle Fuel Efficiency

Shima Nazari[1], Robert J. Middleton[1], Jason Martz[1] and Anna G. Stefanopoulou[1]

Abstract— **High fuel economy is typically achieved with smooth velocity profiles, which can be attained with slow engine response. The reverse however, is not true. Specifically, this paper shows that slow engine response may have deleterious fuel economy effects when aggressive profiles such as the US06 drive cycle need to be tracked. This effect is crucial for strategies which enable higher fuel efficiency at the expense of engine responsiveness. It is shown that slow engine dynamics lead to fluctuations in vehicle tracking performance that result in higher fuel consumption. The effect is quantified with a mean value model of a vehicle with a turbocharged engine undergoing the US06 drive cycle with two different strategies, trading off fuel economy and turbo-lag. The strategies include one that minimizes the engine backpressure through wastegate control (MBWG) and another that uses low pressure loop cooled exhaust gas recirculation (LP-cEGR) in addition to the MBWG strategy. The results indicate that slower engine dynamics can completely overshadow (in the LP-cEGR case) or even reverse (in the MBWG case) these strategies' fuel economy gains.**

I. INTRODUCTION

Powertrain systems are becoming more and more complex to meet increasingly stringent government fuel economy regulations. Turbocharging and downsizing, hybridization and alternative combustion modes are all some of the state of the art methods for enhancing vehicle fuel economy. Unfortunately, these strategies can decrease engine fuel consumption at the expense of engine responsiveness. For example, the fuel economy of turbocharged gasoline engines can be improved through wastegate control strategies that minimize engine pumping losses. However, this approach may degrade the engine responsiveness due to the lower available boost pressure [1].

Another strategy that enables higher fuel economy in turbocharged gasoline engines is cooled Exhaust Gas Recirculation (cEGR). cEGR improves the engine brake efficiency by lowering pumping and heat transfer losses, enabling Maximum Brake Torque (MBT) combustion phasing and the avoidance of fuel enrichment at high loads [2], [3], [4]. However, this practice slows the air path dynamics of the engine by more than 1 second during a large tip-in with 15% cEGR [5].

Although low engine responsiveness is usually synonymous with poor vehicle drivability, it can also affect fuel economy when considering the vehicle-driver-powertrain system performance during the drive cycle. Engine dynamics influence vehicle tracking performance, and the driver might have to change aggressiveness according to the engine dynamics. The driver aggressiveness effect on increasing the vehicle fuel consumption is well known for a fixed engine response [6], [7], while this paper focuses on the impact of slower engine dynamics on vehicle drive cycle fuel economy.

Note that this work investigates how the engine dynamics affect the driver-vehicle system interaction and the associated fuel consumption variation. It is not to be confused with the correction often included in steady-state maps to derive fuel consumption during transients [8]. These two effects are different and modifying the static engine fueling map for transient operation can be still pursued for a more accurate real-world efficiency. The US06 drive cycle is selected for this study because it is part of the EPA fuel economy ratings and includes more aggressive transients where engine slow dynamics may have a larger influence than the FTP or HWY cycles.

This paper is organized as follows: in the first part, it is shown through linear analysis that slow engine dynamics can cause fluctuations in vehicle tracking performance and make the driver behave more aggressively (similar to a high gain controller applied to a slow system in the prototypical feedback system of Fig. 1) when targeting a specific acceleration profile, which leads to even higher speed oscillations. In the second part, the impact of vehicle speed fluctuations on fuel economy is discussed. Finally, the paper concludes by discussing the effect of slow engine dynamics associated with a low backpressure wastegate control strategy and a LP-cEGR strategy on the US06 fuel economy.

II. LINEAR ANALYSIS

When following a trajectory the driver actuates the gas or brake pedal based on a preview of the traffic ahead and the distance from leading vehicles. If the vehicle speed should be decreased, the driver decreases the gas pedal position or applies brakes. Alternatively, if vehicle acceleration is desired, then the gas pedal is depressed to provide the necessary tractive force. However, the powertrain cannot immediately apply this force to the road due to system dynamics and delays, including engine dynamics. If the driver responds impatiently to the lack of acceleration, they will depress the

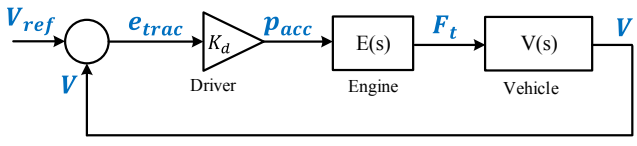

Fig. 1. Simplified linear closed loop model for the vehicle-driver-powertrain system

[1]Department of Mechanical Engineering, University of Michigan, Ann Arbor, MI, USA snazari@umich.edu

pedal beyond the necessary pedal position, which eventually causes higher speed when the engine catches up. Facing the higher speed, the driver retracts the pedal, which can cause a lower than demanded speed. This type of aggressive (high gain) control causes oscillatory tracking in light of a fast tracking signal. This basic linear analysis will be performed first in the following section, followed by a nonlinear simulation.

A. Closed Loop Linear System

This section investigates the effect of engine responsiveness on the tracking performance of the vehicle-driver-powertrain system. In order to use linear analysis techniques, simplified first order linear time invariant (LTI) models are assumed for the engine and the vehicle while the driver is assumed to be a proportional controller with gain K_d. Fig.1 shows this closed loop linear system. In later sections more complex vehicle dynamics are used for simulation and quantifying the impact on fuel consumption. The assumed engine, $E(s)$, and the vehicle, $V(s)$, LTI models are as follows:

$$E(s) = \frac{K_e}{\tau_e s + 1} \tag{1}$$

$$V(s) = \frac{K_v}{\tau_v s + 1} \tag{2}$$

where K_e is the DC gain of the engine LTI model and is the maximum available tractive force of the powertrain. The engine first order time constant, τ_e, depends on the engine technology (naturally aspirated, turbocharged, supercharged, etc).

The vehicle LTI model, $V(s)$, is acquired by applying system identification to a nonlinear vehicle model during a transient that is introduced in Fig. 3b. The first order vehicle time constant, τ_v, was identified as 104 seconds. The nonlinear vehicle model is defined with (3) and (4):

$$M_v \dot{V} = F_t - F_r \tag{3}$$

$$F_r = C_{r,0} + C_{r,1} V + C_{r,2} V^2 \tag{4}$$

where M_v is the vehicle mass, V is the vehicle speed, F_t is the tractive force and F_r is the road resistance force. The terms in (4) correspond to the rolling resistance force and aerodynamic drag force. $C_{r,0}$, $C_{r,1}$ and $C_{r,2}$ are chassis dynamometer correction factors from EPA reported values [9] for a MY2015 Ford Escape given in Table I. The vehicle weight is the EPA reported test weight for this vehicle and the tire radius is the manufacturer reported value. Lumping all proportional gains into one parameter, K, the closed loop transfer function, $T(s)$ is:

$$T(s) = \frac{K}{\tau_e \tau_v s^2 + (\tau_e + \tau_v) s + K + 1} \tag{5}$$

$$K = K_d K_e K_v \tag{6}$$

The effect of engine dynamics and driver aggressiveness on the tracking performance of system (5) are investigated and discussed in the following sections.

TABLE I
VEHICLE PARAMETERS FOR MY2015 FORD ESCAPE [9]

Vehicle Attribute	Value	Units
Test Weight	1758	kg
Tire Radius	431.8	mm
$C_{r,0}$	97.33	N
$C_{r,1}$	4.0349	Ns/m
$C_{r,2}$	0.4970	$\mathrm{Ns}^2/\mathrm{m}^2$

B. Engine Dynamics Effect

The closed loop response of system (5) is investigated here for a fixed driver gain, K_d, hence fixed open loop gain K. Fig. 2b shows the variation of the closed loop damping ratio versus the engine time constant (blue). A range of representative numbers are used for τ_e in this section (from 0.1 to 1 second) for different engine dynamics varying from a naturally aspirated to a turbocharged engine equipped with cooled exhaust gas recirculation, see the turbocharged engine with cEGR dynamic response plot on Fig. 9. The open loop DC gain, K, is assumed to be equal to 80 for computing these results (shown on Fig. 2a). The closed loop system damping ratio drops as the engine responsiveness drops, which implies that even at constant driver gain (fixed driver behavior) system (5) tracking becomes oscillatory when the powertrain dynamic response becomes too slow. Fig. 2c shows the step response overshoot of system (5) versus τ_e. The overshoot increases as the engine dynamic response becomes slower.

C. Driver Effect

The tracking performance of system (5) is studied to understand how driver aggressiveness impacts vehicle tracking performance for a selected portion of the US06 drive cycle.

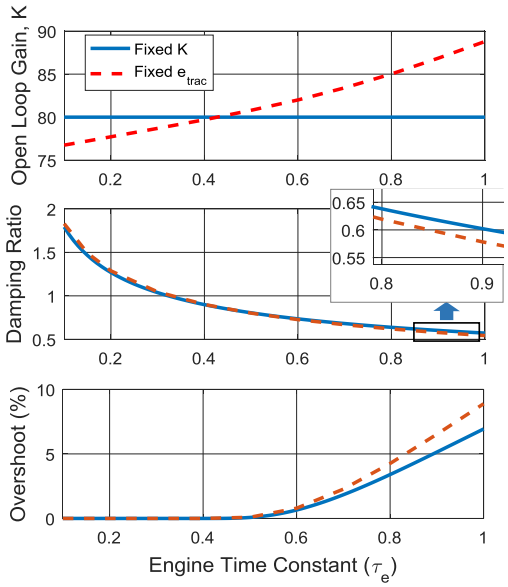

Fig. 2. **(a)** Open loop gain **(b)** Damping ratio of the closed loop system **(c)** Overshoot of the closed loop system to a step input

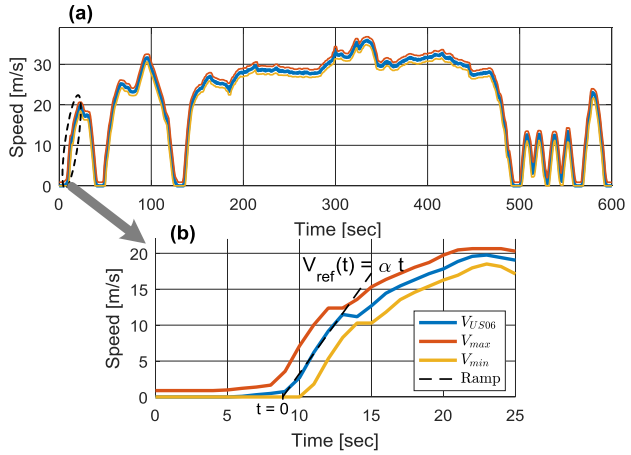

Fig. 3. **(a)** US06 drive cycle speed trajectory **(b)** Studied transient approximated with a ramp profile

Fig. 3a shows the US06 drive cycle speed trajectory and the minimum and maximum allowable speed thresholds. A part of the drive cycle with one of the sharpest accelerations is marked with a black dashed ellipse in Fig. 3a and is magnified in Fig. 3b. The tracking problem is further simplified into following a ramp input, which is shown on the plot by a dashed black line.

The response of system (5) to an input signal of the form $V_{ref}(t) = \alpha t$ can be evaluated analytically. For an underdamped system:

$$V(t) = A_1 + A_2 t + e^{-\frac{\tau_e+\tau_v}{2\tau_e\tau_v}t}\Big(A_3\cos(\frac{\eta t}{2\tau_e\tau_v}) + \frac{A_4}{\eta}\sin(\frac{\eta t}{2\tau_e\tau_v})\Big) \quad (7)$$

and for an overdamped system:

$$V(t) = A_1 + A_2 t + A_5 e^{\frac{-(\tau_e+\tau_v+\zeta)t}{2\tau_e\tau_v}} + A_6 e^{\frac{-(\tau_e+\tau_v-\zeta)t}{2\tau_e\tau_v}} \quad (8)$$

where $V(t)$ is the vehicle speed and,

$$\Delta = \tau_e^2 + \tau_v^2 - 2\tau_e\tau_v - 4K\tau_e\tau_v \quad (9)$$

$$\eta = \sqrt{-\Delta} \quad (10)$$

$$\zeta = \sqrt{\Delta} \quad (11)$$

$$A_1 = -\frac{(\tau_e+\tau_v)\alpha K}{(K+1)^2} \quad (12)$$

$$A_2 = \frac{\alpha K}{K+1} \quad (13)$$

$$A_3 = \frac{(\tau_e+\tau_v)\alpha K}{(K+1)^2} \quad (14)$$

$$A_4 = \alpha K\Big(\frac{(\tau_e+\tau_v)^2}{(K+1)^2} - \frac{2\tau_e\tau_v}{K+1}\Big) \quad (15)$$

$$A_5 = \frac{K\alpha}{K+1}\Big(\frac{\tau_e\tau_v}{\zeta} - \frac{(\tau_e+\tau_v)(\tau_e+\tau_v+\zeta)}{2\zeta(K+1)} + \frac{\tau_e+\tau_v}{K+1}\Big) \quad (16)$$

$$A_6 = \frac{K\alpha}{\zeta}\Big(\frac{(\tau_e+\tau_v)(\tau_e+\tau_v+\zeta)}{2(K+1)^2} - \frac{\tau_e\tau_v}{K+1}\Big) \quad (17)$$

The vehicle tracking error, $e_{trac} = V_{ref}(t) - V(t)$, can be computed using (7) to (17). For the transient studied here, the minimum and maximum speed thresholds are represented on Fig. 3b. The required open loop gain, K, can be calculated for different engine first order time constants (τ_e) assuming that the tracking error is equal to the maximum allowable error at the end of the ramp profile. Fig. 2a (dashed red) shows the resulting K variation versus τ_e, and indicates that as the engine responsiveness deteriorates, (via a larger τ_e) the open loop gain has to be higher to achieve tracking. Note that the open loop gain defined in (6) is the product of the driver gain, K_d, the vehicle gain, K_v and the engine gain, K_e. The latter two gains, K_v and K_e are constant in this study so higher open loop gain means higher driver gain, which implies that the driver has to be more aggressive in order to achieve tracking. This effect further decreases the damping ratio of the closed loop system (shown as the dashed red line in Fig. 2b) and increases the system overshoot, shown in Fig. 2c.

The linear analysis presented in this section indicates that low engine responsiveness can increase the tracking oscillations of the vehicle-driver-powertrain system, while a slow engine requires the driver to behave more aggressively in order to track a specific drive cycle speed profile, which further decreases the closed loop damping ratio and in turn increases tracking oscillations. Including nonlinear effects in the model shown in Fig. 1, such as the driver delay (the time that the driver needs to respond to the input signal) or saturation on the driver signal to the powertrain (the driver cannot command a pedal position greater than 100%), will cause the overshoot in closed loop response to increase beyond what is shown in Fig. 2.

III. SPEED FLUCTUATIONS EFFECT ON FUEL CONSUMPTION

In the previous section it was shown that slow engine dynamics lead to tracking oscillations in the vehicle-driver-powertrain system. This section investigates the impact of speed fluctuations on vehicle fuel consumption. In an internal combustion engine, the Brake Specific Fuel Consumption (BSFC) is defined as:

$$\text{BSFC} = \frac{\dot{m}_f}{P_b} \quad (18)$$

$$P_b = T_e\omega_e \quad (19)$$

where $\dot{m}_f$ is the fuel mass flow rate, P_b is the engine brake power, T_e is the engine brake torque and ω_e is the engine angular speed. The tractive force, F_t, and the engine

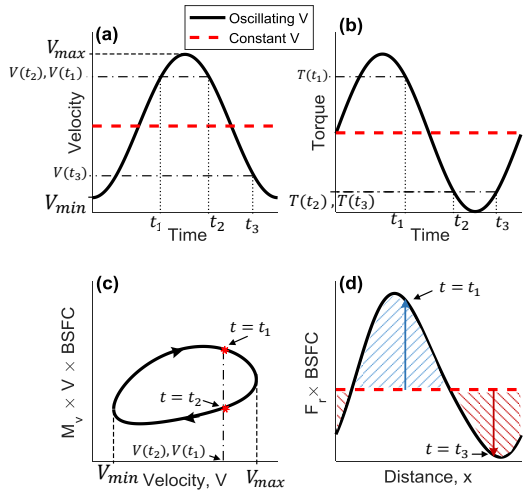

Fig. 4. **(a)** Velocity profile **(b)** Torque profile **(c)** Fuel consumed for acceleration **(d)** Fuel consumed for road load

brake torque are related as follows, assuming a locked torque converter and negligible drivetrain losses:

$$F_t = T_e \frac{n_g n_{fd}}{R_w} \tag{20}$$

where n_g is the transmission gear ratio, n_{fd} is the final drive ratio and R_w is the tire radius. Equations (3) and (4) define the relationship between tractive force, vehicle acceleration and resisting forces on the vehicle. Assuming that the vehicle is not braking and combining (3) to (4) and (18) to (20) results in the following expression for the engine fuel flow rate:

$$\dot{m}_f = (M_v V \dot{V} + C_{r,2} V^3 + C_{r,1} V^2 + C_{r,0} V)\text{BSFC} \tag{21}$$

Integrating the above equation over some velocity profile, $\tilde{V}$, and associated travel distance, 0 to $\tilde{x}$, results in the following expression for the consumed fuel mass, m_f:

$$m_f = \oint^{\tilde{V}} M_v V \text{BSFC} dV + \int_0^{\tilde{x}} (C_{r,2} V^2 + C_{r,1} V + C_{r,0})\text{BSFC} dx \tag{22}$$

The first term in (22) corresponds to the fuel consumed due to vehicle's kinetic energy change, while the second term accounts for the fuel consumed to overcome vehicle rolling resistance and drag.

It is important to find the sufficient condition for an increase in fuel consumption associated with each term of (22) due to vehicle speed fluctuations. Fig. 4a shows two velocity profiles with equal mean values and distance traveled, one with a constant speed (dashed red) and the other with a fluctuating speed profile (black). Presume that the speed fluctuation is small compared to the mean value but the acceleration is non-negligible (which is similar to the vehicle speed fluctuations discussed in this study). Fig. 4b shows the torque profile associated with both speed profiles in Fig. 4a (computed through (3), (4) and (20).) Due to the prevailing vehicle acceleration term the engine torque will be higher during accelerating compared to decelerating.

Fig. 4c shows a schematic of the integrand of the first term in (22) versus vehicle velocity for the "Oscillating V" speed profile shown in Fig. 4a and b. The area enclosed by the ellipse shaped curve will be the increase (if the curve is clockwise) or the decrease (if the curve is counterclockwise) in vehicle fuel consumption. The sufficient condition for the curve to have a clockwise direction is that at any arbitrary times t_1 and t_2 that have equal speed but different acceleration signs, the value of the integrand ($M_v \times V \times$ BSFC) be higher for time t_1, when the vehicle is accelerating. As shown in Fig. 4b the engine torque is higher during acceleration, ($T(t_1) > T(t_2)$) and since M_v is constant and $V(t_1) = V(t_2)$, BSFC(t_1) must be greater than BSFC(t_2), or the engine BSFC should be increasing in the engine torque to have a higher fuel consumption due to vehicle speed fluctuations associated with the first term in (22).

Fig. 4d shows the integrand of the second term in (22) versus the distance traveled. To have a higher fuel consumption associated with this term compared to the constant speed case, the area of the blue cross-hatched part should be larger than the area of the red cross-hatched part. The sufficient condition for this is that for any arbitrary points the average value of the integrand, $F_r \times$ BSFC, at these points should be higher than its value at the average point. For example the average of points t_1 and t_3 shown on the figure correspond to the "Constant V" case and the average of the integrand at these points (deviations from the "Constant V" case are shown with arrows for both points, and the blue arrow is longer than the red one) should be higher than the integrand value for the average point (red line) which is the case here. This condition is equivalent to convexity of the integrand.

Whether the vehicle speed fluctuations related to the first term in (22) lead to higher or lower fuel consumption depends on the operating point of the engine and whether the engine BSFC is increasing or decreasing with torque at this point. This very same fact motivated researchers to design vehicle control strategies that save fuel through fluctuating between the idle and best efficiency point of the engine, known as pulse and glide [11], [12]. However, the oscillations discussed in this study are a consequence of slow engine dynamics. For turbocharged engines, the slow engine dynamics are associated with lags in air system under boosted conditions. Fig. 5a shows a 1.6 liter 2013 EcoBoost engine BSFC map ([10], republished with permission) and Fig. 5b shows the US06 drive cycle visited points and their residence time on the same engine map. Although most of the engine operating points lie between 1500 to 2500 rpm and 50 to 150 Nm engine torque, the speed-torque trajectories where sluggish engine response causes oscillation in the vehicle tracking performance lie approximately between 1500 to 4000 rpm and above 110 Nm torque. In this area, the engine BSFC map has little variation with torque (the green area in Fig. 5a) or has positive gradients versus torque (the area above the green area in Fig. 5a). This means that fluctuations originating from slow turbocharged engine

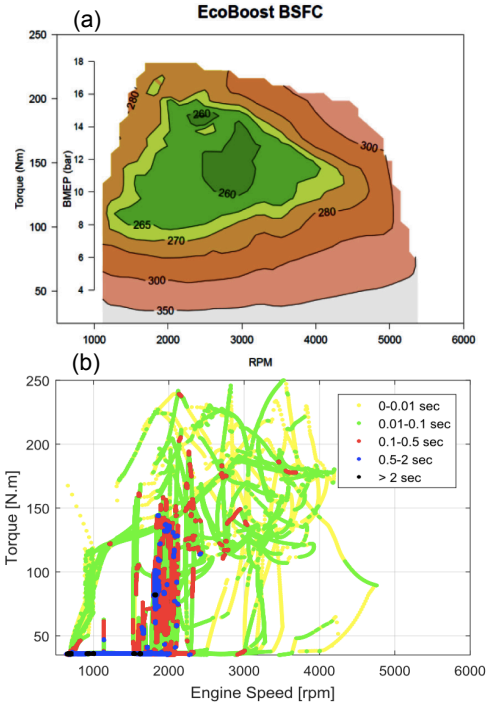

Fig. 5. **(a)** 1.6 L Ecoboost engine BSFC map [10] **(b)** Visited points and their residence time for Ford Escape in the US06 drive cycle

dynamics will most likely increase fuel consumption during vehicle acceleration.

The sufficient condition for having an increasing relation between vehicle speed fluctuations and the fuel consumption associated with the second term in (22) is the convexity of the integrand ($F_r \times$ BSFC function) in the high torque map area described above (with engine speed from 1500 to 4000 rpm and torque higher than 110 Nm) and generalize the results due to similarity in the shape of the turbocharged engines BSFC map. Since the engine BSFC map is not smooth, it is replaced with a second order polynomial (BSFC$_{fitted}$) that approximates the actual map (mean absolute error 3 g/kWh) and the convexity of the resulting smooth function $F_r \times$ BSFC$_{fitted}$ is studied. This approach clarifies the general effect of vehicle speed oscillations without having to deal with local behavior arising from BSFC map variabilities. Fig. 6 shows the $F_r \times$BSFC$_{fitted}$ versus engine torque and speed, assuming operation in fifth gear, the result will be similar for other gears. The convex shape of the function can be inferred from the represented contour lines.

The goal of this section was to clarify the impact of vehicle tracking performance on fuel consumption. The results show that at the operating conditions where low engine responsiveness causes oscillations in vehicle speed, both fuel consumption terms of the vehicle per (22), one associated with vehicle acceleration and the other associated with vehicle road load, increase as fluctuations in vehicle speed and engine torque grow. So the tracking fluctuations caused by a slow turbocharged engine can lead to higher vehicle fuel consumption.

IV. DRIVE CYCLE SIMULATION

It was shown that fluctuations in the vehicle speed arising from low turbocharged engine responsiveness at boosted conditions can increase the vehicle fuel consumption. In this section this effect is quantified for a vehicle with turbocharged engine and different calibrations over the US06 drive cycle.

A. Vehicle, Engine and Driver Model

The baseline vehicle selected for this study is a MY2015 Ford Escape with a 4 cylinder 1.6 L EcoBoost engine and 6 speed automatic transmission. The vehicle and transmission, including the gearbox, torque converter and lock up clutch, are modeled in GT-Suite [13], while the engine and driver are modeled in MATLAB Simulink. The vehicle physical parameters are reported in Table I. The automatic transmission shift strategy is based on accelerator pedal position and engine speed, as detailed by Middleton et. al. [14]. The torque converter is locked in 1st and 2nd gear when above 1000 rpm engine speed, and for the other gears at all speeds above idle.

Fig. 7 shows the layout of the model and the interaction of the sub-models. The driver, which is a proportional controller, determines the brake pedal and accelerator pedal position according to the tracking error. The GT-Suite model computes vehicle speed and engine speed using the engine produced torque, accelerator and brake pedal position. The engine block is a mean value engine model (MVM) for a 1.6 L Ford EcoBoost gasoline turbocharged direct injection (GTDI) engine equipped with LP-cEGR. The MVM calculates the engine torque for a commanded accelerator pedal position and current engine speed.

The MVM states include: boost pressure, intake manifold pressure, exhaust manifold pressure and turbocharger inertia. In the model a reference intake manifold pressure is determined using a 2D map based on engine speed and pedal position. A reference boost pressure is then selected using the reference intake manifold pressure and a desired pressure drop across the throttle. A PI controller actuates the throttle position to target the intake manifold pressure while a second PI controller moves the wastegate to target the reference boost pressure [5]. Fig. 9 shows the closed loop

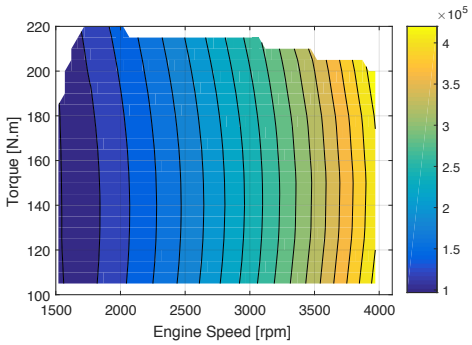

Fig. 6. 2D contour of resistance force $\times$ BSFC$_{fitted}$

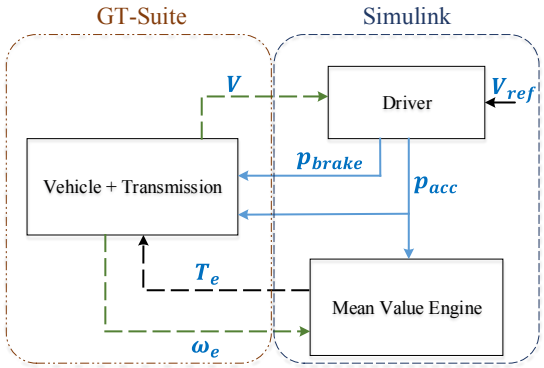

Fig. 7. Model layout and interaction of its sub-models

torque response of the MVM at a constant engine speed of 2000 rpm, for three different cases:

- "TC-fast" (red) is the turbocharged engine with a boost pressure of 0.2 bar higher than the minimum required boost pressure (introduced below) and no cEGR. The engine responsiveness is high in this case because of the reserved boost pressure.
- "TC-MBWG" (dashed yellow) is the turbocharged engine with a minimum boost pressure (which is equal to the intake manifold pressure for boosted conditions and ambient for non-boosted conditions). This strategy is called "minimum back pressure wastegate control" (MBWG). Engine responsiveness deteriorates in this case due to less accumulated boost pressure before the throttle valve. This case is also without cEGR.
- "TC-cEGR+MBWG" (dashed dotted purple) is the turbocharged engine with 15% low pressure cEGR and the MBWG strategy. The engine responsiveness is the slowest of the three engine calibrations considered as the result of the lower reserved boost pressure, partial pressure of exhaust gases in the air path and decreased specific enthalpy of exhaust gases, given the lower exhaust temperatures of this strategy.

The MVM model successfully captures the nonlinear turbocharged engine dynamics and was validated against high fidelity GT-power simulations for the same engine under study, described in detail in the previous work [5].

B. Results

Table II summarizes the fuel consumption (FC) results for the "MBWG" and "cEGR+MBWG" strategies compared to the baseline engine with fast throttle/wastegate coordination ("TC-fast" above). In each case the driver gain is chosen as the minimum necessary value to follow the drive cycle while the same gear shift strategy is used for all cases.

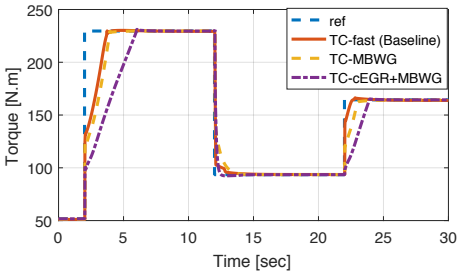

Fig. 8. Mean value engine model closed loop torque response

TABLE II
FORD ESCAPE FUEL CONSUMPTION COMPARISON OVER US06 DRIVE CYCLE WITH DIFFERENT ENGINE STRATEGIES

Strategy	Steady State FC Effect	Engine Dynamics FC Effect	Net FC Effect	MPG
Baseline	0.0%	0.0%	0.0%	25.53
MBWG	−0.8%	1.1%	0.3%	25.45
cEGR +MBWG	−3.7%	3.1%	−0.6%	25.68

The steady state fuel consumption effect of the "MBWG" and "cEGR+MBWG" strategies (first column in Table II) were derived for the same engine by authors in a previous study [5]. The results indicated that the MBWG strategy decreases the engine fuel consumption 0.8% and if a 15% cEGR strategy was employed too, the fuel consumption would drop by 3.7% for low to medium loads.

Engine dynamics fuel consumption effects (second column in Table II) are examined by simulating the US06 drive cycle using the same 2D lookup table of experimental fueling rate based on instantaneous engine speed and torque for all cases to isolate the engine responsiveness impact on fuel consumption and fuel economy. The results show that a deterioration in engine responsiveness similar to the "MBWG" strategy could cause a 1.1% increase in fuel consumption over the US06 drive cycle. Considering both effects of decreased fuel consumption due to minimizing engine pumping losses, and increased fuel consumption arising from slower dynamics, the net effect of MBWG over the US06 drive cycle would be 0.3% higher fuel consumption than the baseline engine with more pumping losses but faster response. The simulations also indicate that the slow engine dynamics similar to the "cEGR+MBWG" strategy can contribute to a 3.1% increase in fuel consumption. Subtracting this number from the steady state fuel consumption decrease of the strategy, the net effect could be only a 0.6% decline in fuel consumption, which is less than 20% of the initial expected drop. This highlights the necessity of including secondary strategies to increase engine responsiveness, such as variable speed supercharging [15], electrical turbocharging [16] and torque assist. Without such features vehicle drivability can suffer, while fuel economy gains will be smaller than expected.

Fig. 9 compares the tracking performance of the turbocharged engine with fast throttle/wastegate coordination ("TC-fast", blue line) to the turbocharged engine with cEGR ("TC-cEGR+MBWG", dashed red line) during two segments of the US06 drive cycle and their associated instantaneous fueling rates. The slightly higher vehicle speed fluctuations for the case with the slower engine (TC-cEGR+MBWG) is noticeable in Fig. 9a and Fig. 9b. Fig. 9c and Fig. 9d

show how these small speed fluctuations result in higher fueling rates. The consumed fuel in a specific interval is the time integral of instantaneous fuel rate (the area bellow the plot). Although the instantaneous fueling rates of the "TC-fast" and "TC-cEGR+MBWG" are different but in both intervals the consumed fuel of the "TC-cEGR+MBWG" is higher. As mentioned before the same static fueling maps are used in producing these plots and is not compensated for the engine transient fuel flow rate deviation. Applying the transient compensation might change the absolute value of the reported numbers but the trend should last.

V. CONCLUSION AND FUTURE STUDY

Small signal analysis of the vehicle-driver-powertrain system indicates that a vehicle with a slow engine can have more velocity fluctuations when following a drive cycle due to both low engine responsiveness and a necessary higher gain driver. The speed and torque fluctuations arising from the low responsiveness of turbocharged engines can increase vehicle fuel consumption. This results from the lower efficiency of the engine under high boost conditions and the convexity of road load with respect to the vehicle speed. The effect was quantified for two engine strategies undergoing the US06 drive cycle; one with minimum backpressure wastegate control (MBWG) and the other with low pressure cooled EGR and MBWG (LP-cEGR+MBWG). For the MBWG strategy, fuel economy can be lower relative to a strategy that reserves boost pressure for faster transients, and for the LP-cEGR+MBWG strategy, less than 20% of the expected fuel consumption drop was gained. This result highlights the importance of engine responsiveness to fuel economy during an aggressive drive cycle like the US06. Specifically, it indicates that when vehicle and driver performance in a drive cycle is considered, slow engine dynamics can change the predicted fuel economy gain of strategies that trade off fuel economy and engine responsiveness such as MBWG and LP-cEGR.

Future work will study the impact of drive cycle aggressiveness and driving style on the fuel consumption increase arising from low engine responsiveness. Given that slow engine dynamics do not result in fuel economy decrease for every driving profile, these effects will most likely be small when tracking a smooth driving profile.

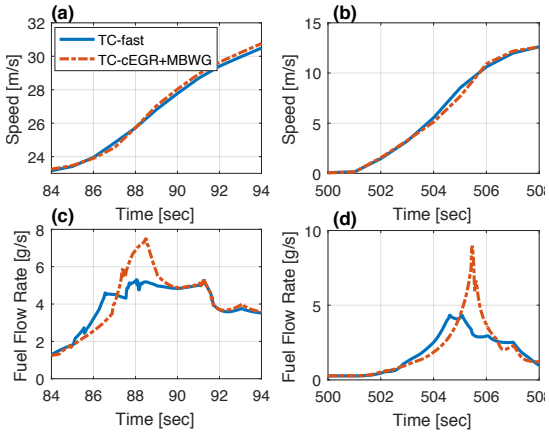

Fig. 9. Tracking performance of fast turbocharged and turbocharged engine with cEGR and associated fueling rates during two segments of the US06 drive cycle

VI. ACKNOWLEDGEMENT

The information, data, or work presented herein was funded in part by the Advanced Research Projects Agency-Energy (ARPA-E), U.S. Department of Energy, under Award Number DE-AR0000659. The views and opinions of authors expressed herein do not necessarily state or reflect those of the United States Government or any agency thereof.

REFERENCES

[1] L. Eriksson, S. Frei, C. Onder, and L. Guzzella, "Control and optimization of turbo charged spark ignited engines," in *IFAC world congress*, 2002.

[2] D. Takaki, H. Tsuchida, T. Kobara, M. Akagi, T. Tsuyuki, and M. Nagamine, "Study of an egr system for downsizing turbocharged gasoline engine to improve fuel economy," SAE Technical Paper, Tech. Rep., 2014.

[3] L. Teodosio, V. De Bellis, and F. Bozza, "Fuel economy improvement and knock tendency reduction of a downsized turbocharged engine at full load operations through a low-pressure egr system," *SAE International Journal of Engines*, vol. 8, no. 4, pp. 1508–1519, 2015.

[4] L. Francqueville and J.-B. Michel, "On the effects of egr on spark-ignited gasoline combustion at high load," *SAE International Journal of Engines*, vol. 7, no. 4, pp. 1808–1823, 2014.

[5] S. Nazari, J. Martz, and A. Stefanopoulou, "Minimum backpressure wastegate control for a boosted gasoline engine with low pressure external egr," in *ASME 2016 Dynamic Systems and Control Conference*. American Society of Mechanical Engineers, 2016.

[6] S. Lee, J. Choi, K. Jeong, and H. Kim, "A study of fuel economy improvement in a plug-in hybrid electric vehicle using engine on/off and battery charging power control based on driver characteristics," *Energies*, vol. 8, no. 9, pp. 10 106–10 126, 2015.

[7] Z. Liu, A. Ivanco, and Z. S. Filipi, "Impacts of real-world driving and driver aggressiveness on fuel consumption of 48v mild hybrid vehicle," *SAE International Journal of Alternative Powertrains*, vol. 5, no. 2016-01-1166, pp. 249–258, 2016.

[8] N. Mizushima, K. Yamaguchi, D. Kawano, H. Suzuki, and H. Ishii, "A study on high-accuracy test method for fuel consumption of heavy-duty diesel vehicles considering the transient characteristics of engines," *SAE International Journal of Fuels and Lubricants*, vol. 9, no. 2016-01-0908, pp. 383–391, 2016.

[9] U. E. P. Agency. 2015 fuel economy datafile. [Online]. Available: http://www.fueleconomy.gov/feg/download.shtml

[10] M. Stuhldreher, C. Schenk, J. Brakora, D. Hawkins, A. Moskalik, and P. DeKraker, "Downsized boosted engine benchmarking and results," SAE Technical Paper, Tech. Rep., 2015.

[11] J. Lee, "Vehicle inertia impact on fuel consumption of conventional and hybrid electric vehicles using acceleration and coast driving strategy," 2009.

[12] S. E. Li, H. Peng, K. Li, and J. Wang, "Minimum fuel control strategy in automated car-following scenarios," *IEEE Transactions on Vehicular Technology*, vol. 61, no. 3, pp. 998–1007, 2012.

[13] Gamma Technologies, Inc., Westmont, IL, "Gt-suite v7.4." [Online]. Available: http:// www.gtisoft.com

[14] R. J. Middleton, O. G. H. Gupta, H.-Y. Chang, G. Lavoie, and J. Martz, "Fuel efficiency estimates for future light duty vehicles, part b: Powertrain technology and drive cycle fuel economy," SAE, No. 2016-01-0905, Tech. Rep., 2016.

[15] S. Nazari, R. Kiwan, and A. Stefanopoulou, "A coordinated boost control in a twincharged spark ignition engine with high external dilution," in *ASME 2016 Dynamic Systems and Control Conference*. American Society of Mechanical Engineers, 2016.

[16] I. Kolmanovsky, A. Stefanopoulous, and B. Powell, "Improving turbocharged diesel engine operation with turbo power assist system," in *Control Applications, 1999. Proceedings of the 1999 IEEE International Conference on*, vol. 1. IEEE, 1999, pp. 454–459.